Scanning Curves in Wedge Pore with the Wide End Closed: Effects of Temperature

Nikom Klomkliang
School of Chemical Engineering, University of Queensland, St. Lucia, QLD 4072, Australia

Faculty of Engineering, Chemical Engineering Program, Naresuan University, Phitsanulok 65000, Thailand

Duong D. Do and David Nicholson
School of Chemical Engineering, University of Queensland, St. Lucia, QLD 4072, Australia

DOI 10.1002/aic.14905
Published online July 1, 2015 in Wiley Online Library (wileyonlinelibrary.com)

The desorption scanning curves within the hysteresis loop of argon adsorbed in a wedge-shaped pore with its wide end closed have been studied in the temperature range between 60 and 87 K, using grand canonical Monte Carlo simulation. The distinct features are: (1) adsorbate packing follows a sequence of commensurate regions (zones) and incommensurate regions (junctions); (2) the mechanism for evaporation switches from cavitation-like pore blocking to cavitation when the temperature is increased; as typically observed for ink-bottle pores. When cavitation is the operating mechanism, the descending scanning curve spans across the loop in two stages: a gradual decrease in density in a zone followed by a sharp evaporation from a junction, and then terminates at the lowest point on the vertical cavitation boundary. The adsorption scanning curve proceeds across the loop in two stages complementary to the desorption scanning-curve: a gradual change in density at a junction followed by a sharp change through a zone. Conversely, when cavitation-like pore blocking is operating, the descending curve leaves the adsorption boundary, spans across the hysteresis loop and returns to a different point on the same boundary, rather than to the desorption boundary or to the lower closure point. This feature does not seem to have been recognized in earlier literature and should be considered in the classification of scanning curves. *AIChE J*, 61: 3936–3943, 2015
Keywords: adsorption, desorption, hysteresis, scanning curve, Monte Carlo simulation, wedge pore, cavitation, pore blocking

Introduction

Hysteresis associated with capillary condensation and evaporation in porous materials has been the subject of immense interest for over 100 years.[1] The hysteresis loop has been regarded as a finger-print for the determination of the structure of a given porous solid; the connectivity of porous solids may be determined from adsorption–desorption boundaries as suggested by Seaton and others.[2–9] However, it is now known that at a given temperature, solids with different pore structures can exhibit similar hysteresis loops[10–12] and that their shape can change significantly with temperature.[13–16] To probe pore structure more effectively, additional information needs to be obtained, and to this end, scanning across the hysteresis loop is proposed as a means of gaining further insight into the structural parameters of the pore network that cannot be deduced from either the adsorption boundary or the desorption boundary of the hysteresis loop.[17–22] A desorption scanning curve is obtained when the pressure is decreased on the adsorption boundary, before the upper closure point of hysteresis is reached. The analogous reversal in pressure on the desorption boundary, before the lower closure point of hysteresis is reached, is termed an adsorption scanning curve.

An early model referred to as the independent domain theory of sorption hysteresis due to Everett and Smith[23] can account for many experimental hysteresis loops. The main idea of the theory is that each pore space can fill and empty independently of the state of its neighbors. According to this theory, desorption and adsorption scanning curves should cross directly between the adsorption and desorption boundary curves. However, experimental scanning curves do not necessarily follow this simple behavior and can be classified into three broad categories: (1) crossing directly between the boundary curves of the hysteresis loop, (2) converging to the closure point, and (3) returning back to the same boundary[17–19,21,22,24,25] and further insight is needed into the origin of these three types of scanning curve. In our recent study,[26] we studied the scanning curves in a wedge pore with either its narrow end or its wide end closed, to understand the way in which such a simple connectivity (in the form of a linear change in pore size in the axial direction) affects the scanning curve.

Within the last decade, two basic mechanisms have been identified for desorption from an elementary unit in a pore network, consisting of a wide cavity connected to a narrow neck: cavitation

Correspondence concerning this article should be addressed to D.D. Do at d.d.do@uq.edu.au.

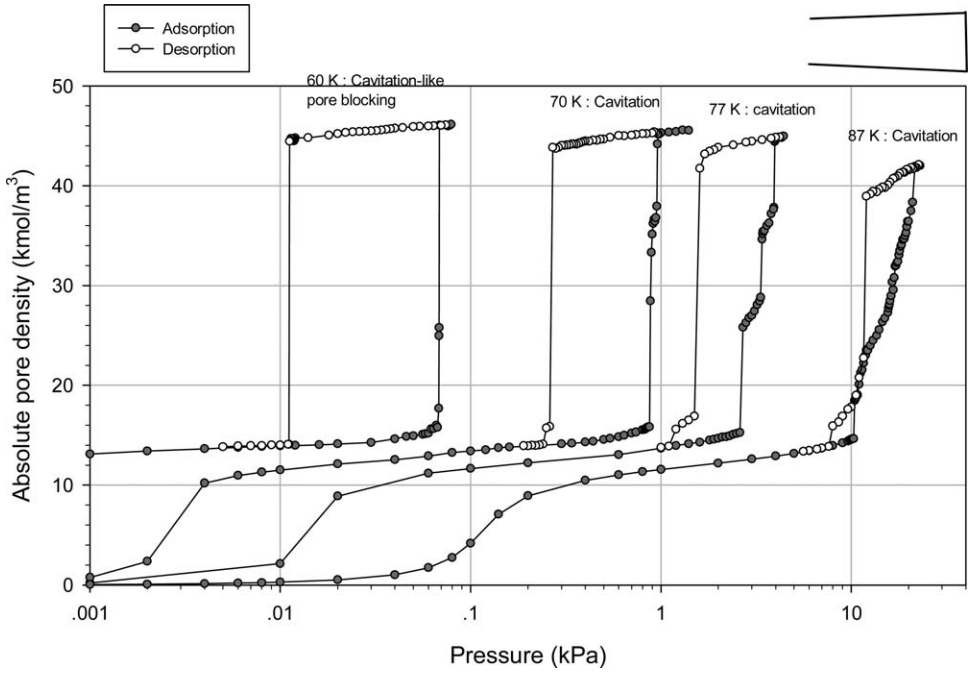

Figure 1. Argon adsorption and desorption isotherms in the wedge pore with its wide end closed at temperatures in the range 60–87 K.

and pore blocking. In the first of these, evaporation occurs from the wide section while the necks remain filled; in the second, molecules in the neck evaporate, resulting in the exposure of the cavity to the bulk gas, and there is consequently an immediate evaporation from the wide section; see references by Sarkisov and Monson, Ravikovithch and Neimark, and Klomkliang et al.[15,16,27] for further discussion. A phenomenon described as cavitation-like pore blocking has also been identified in our previous work[10] as a process in which desorption proceeds via a pore blocking mechanism but the desorption branch shows a steep decrease, even though there is no bubble formation in the cavity.

In this article, we use grand canonical Monte Carlo (GCMC) simulation[28] to investigate the effects of temperature on scanning curves in a wedge pore with its wide end closed where all the phenomena referred to above can be the dominating mechanism of evaporation, depending on conditions. The majority of the previous theoretical work on porous carbons has focussed on models with parallel-sided pores, and models of this type are invariably used as a basis for estimating pore-size distributions. However, it is clear, for example from micrographs, and from reconstructions based on scattering data, that the assumption of parallel-sided pore spaces does not accord well with reality. The simple wedge model in this investigation is an attempt to confront this discrepancy and to examine some of its consequences. We find, as in our previous study of simple wedges, that an extraordinarily rich behavior, and new phenomena associated with scanning across the hysteresis curve emerge. Several previous papers have addressed the problem of fluid adsorption and wetting in wedge geometry both experimentally and theoretically, but hysteresis and scanning have been largely neglected to date.[23,29–31]

Simulation Model and Method

The pore walls and the closed end were modeled as three graphene layers with 0.3354-nm spacing. The axial pore length is 30 nm and the half angle of the wedge was 1.0°. The widths of the narrow and wide ends were 1.953 nm and 3 nm, respectively.

The Lennard Jones 12-6 potential with a collision diameter (σ_{ff}) of 0.3405 nm and energy well-depth (ε_{ff}/k_B) of 119.8 K was used to calculate the intermolecular potential energy in the argon adsorbate. The interaction between argon and the solid adsorbent was calculated from the Bojan–Steele equation[32–34] with the assumption that the lengths in the y and z directions are finite and the length in the x direction is infinite. At least 8×10^8 trial moves were used in the GCMC simulation for each isotherm point of which the first 4×10^8 configurations were used for equilibration and the remaining configurations for computing the ensemble averages (this is an exceptionally large number for simple gases like argon and ensures that each point represents a true equilibrium). Three types of trial moves were attempted with equal probability: displacement, insertion, and deletion. The primary output from a simulation is the ensemble average of absolute volumetric densities (ρ_{pore}^{ABS}), defined by

$$\rho_{pore}^{ABS} = \langle N \rangle / V_{acc} \tag{1}$$

where $\langle N \rangle$ is the ensemble average of the number of particles in the pore and V_{acc} is the accessible pore volume.

Results and Discussion

Wedge pore with the wide end closed

Figure 1 shows the adsorption–desorption isotherms at temperatures between 60 and 87 K for argon in a wedge-shaped pore with its wide end closed. The mechanism of evaporation switches from cavitation-like pore blocking to cavitation when the temperature is increased, behavior typical of ink-bottle pores, where the change in pore size along the axial direction is a step function,[16] and the hysteresis loop changes from type H1 (in the IUPAC classification) at 60 K to a mixture of type H2 (IUPAC) and type C (in the de Boer classification) at 87 K.

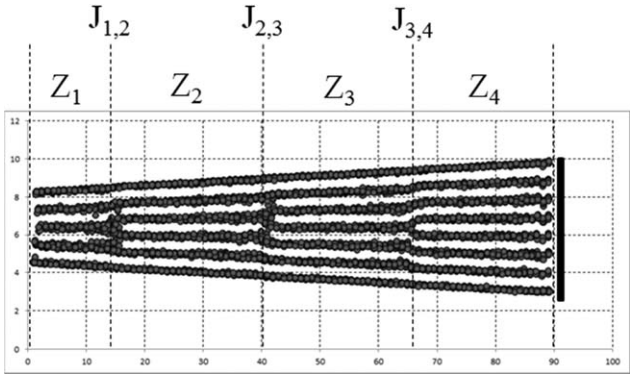

Figure 2. Molecular configurations in zones and junctions in an adsorbate filled wedge pore with wide end closed.

The sequence of sharp jump and gradual change along the adsorption boundary is due to adsorption in various zones along the pore as seen in Figure 2 where we show snapshots of molecules in a completely filled pore. A zone is defined here as the section of the pore where the packing is commensurate across the pore (giving an integral number of molecular layers). A junction is the small region between these zones where the packing becomes incommensurate and we can see the frustration of the adsorbate and bifurcation of the layers in the central part along the axial direction. Hereafter, we shall denote the Zone number i as Z_i and the junction between Zones i and $i + 1$ as $J_{i,i+1}$.

Figure 3 illustrates the adsorption and desorption sequences schematically at different temperatures for reference in the subsequent discussion. The regions where there is a gradual change in density are shaded in gray and those where a sharp change occurs are denoted by arrows. The direction of the arrows indicates the way that adsorbate is added into the pore or adsorbate is removed from the pore at different temperatures.

Cavitation at 70–87 K

For temperatures higher than 70 K, evaporation from a completely filled pore is by cavitation. Figure 4 shows the adsorption–desorption isotherms and their respective scanning curves at

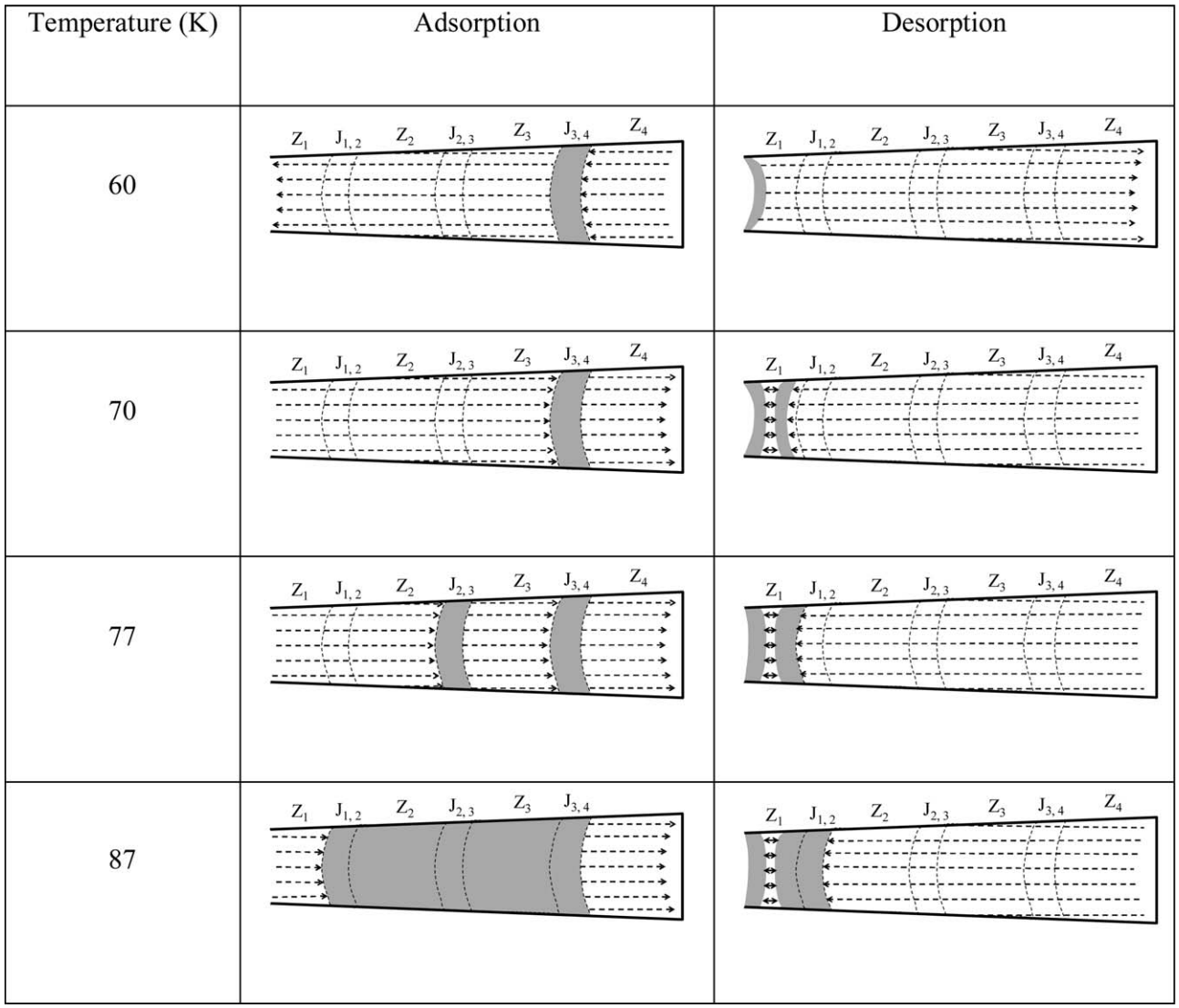

Figure 3. The schematics of adsorption and desorption in the wedge pore at different temperatures.

The gray areas represent the regions where density changes gradually, and the areas with arrows represent the regions where a sharp change in density occurs.

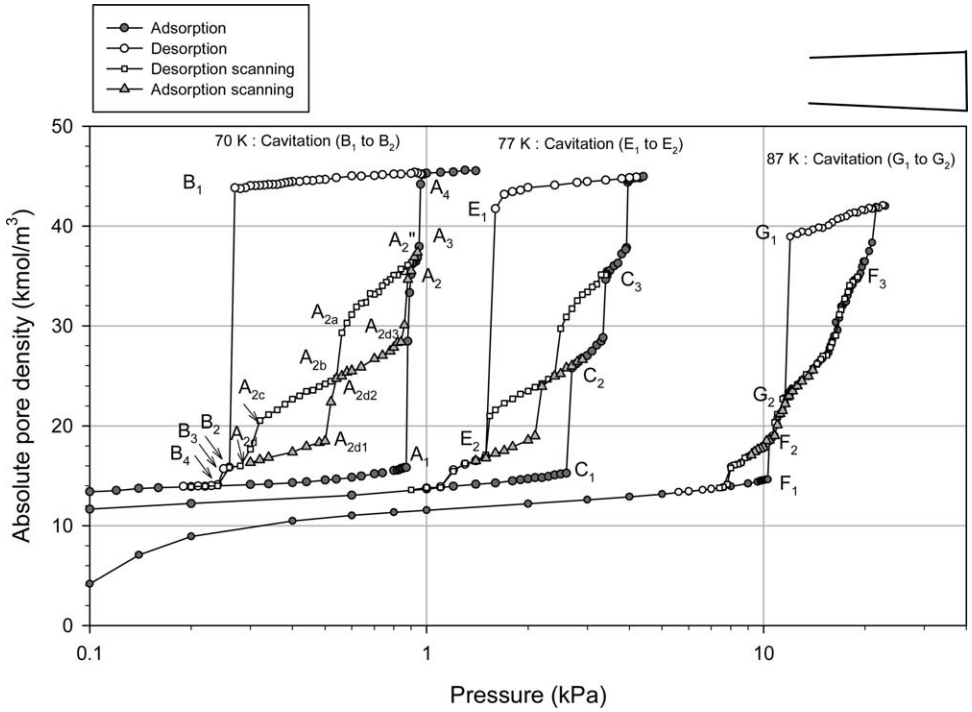

Figure 4. Desorption scanning curve in the wedge pore with wide end closed at 70–87 K.

70, 77, and 87 K. The adsorption and desorption branches behave in a very interesting manner as the temperature is varied. We first discuss the way in which adsorption progresses from an empty pore and desorption proceeds from a completely filled pore which will help in understanding the scanning curves.

70 K. The adsorption branch shows two sharp condensation Segments (A_1A_2 and A_3A_4) separated by a small section

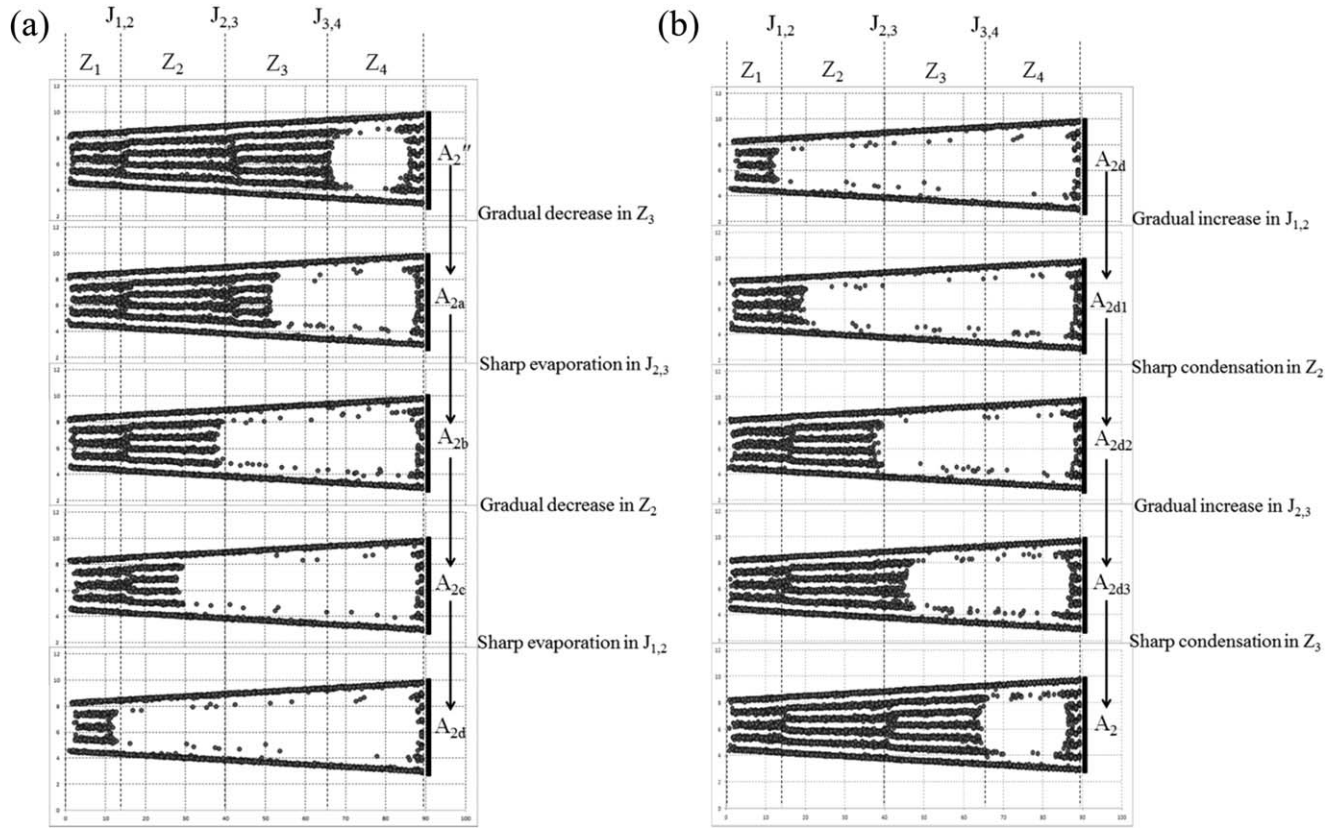

Figure 5. Snapshots in the wedge pore along the desorption scanning curve.

(a) Desorption scanning and (b) adsorption scanning. Points A_2'' to A_{2d} and A_2 are marked on the isotherm in Figure 4.

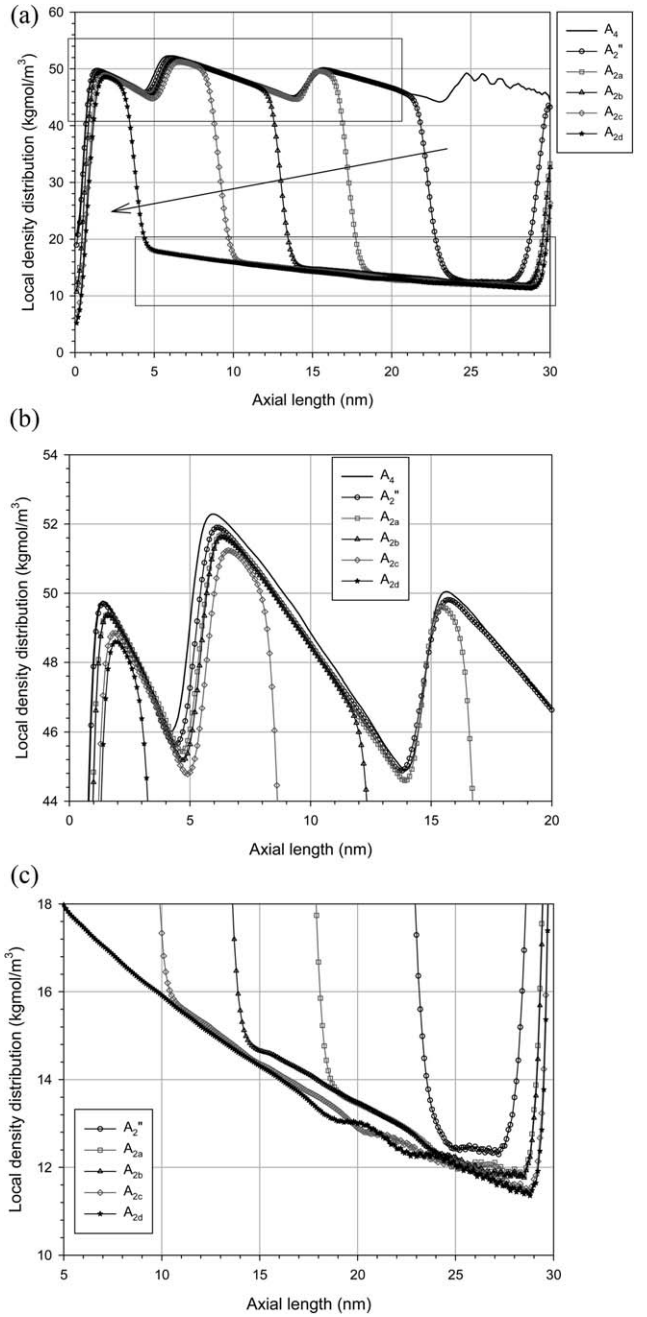

Figure 6. (a) Local density distributions in the wedge pore at 70 K. (b) and (c) are the enlargments of the filled and emptied phases, respectively. Points A''_2 to A_{2d} are marked on the isotherm in Figure 4.

where there is a gradual change in density (A_2A_3). The first step is due to nucleation at the pore mouth, which initiates a sharp condensation in Z_1 to Z_3 (Segment A_1A_2). This is typical of condensation in a wedge pore with a small divergence.[35] This first condensation is followed by gradual filling of the junction between Zones 3 and 4, and is then followed by a sharp condensation in Zone 4, which behaves like a cavity in an ink-bottle pore.

On desorption from a completely filled pore, the wedge pore behaves like an ink-bottle pore and a meniscus recedes from the pore mouth as pressure begins to decrease. As it recedes into the pore interior, the condensate in the interior of the pore is stretched, resulting in a gradual change in the density to Point B_1. As the size of the pore mouth is smaller than the critical width demarcating cavitation from pore blocking at 70 K, the recession of the meniscus is not as significant as the stretching of the adsorbate in the Zones 2–4, and consequently, when the cavitation pressure is reached at Point B_1, a sharp evaporation from these zones occurs. At this point, Zone 1 behaves like an open end wedge pore, and as pressure is further reduced, we see behavior typical of an open end wedge pore (Type C hysteresis, followed by a sharp evaporation, through $B_2B_3B_4$).

Descending scanning is only possible from the state points in the shallow segment of the adsorption boundary (Segment A_2A_3) and detailed discussion about the scanning curves has been reported in our previous work.[26] We start at the point A''_2 where the Junction $J_{3,4}$ is partially filled. When the pressure is decreased, the scanning curve traces this segment until Junction $J_{3,4}$ is emptied, and then spans across the hysteresis loop by exactly the same mechanism as desorption from an open end wedge pore via two distinct processes: (1) gradual decrease from the zone and (2) sharp evaporation from the junction, that is,

a. gradual decrease in density in Zone 3, followed by
b. sharp evaporation from the Junction $J_{2,3}$, and
c. gradual decrease in Zone 2, and
d. sharp evaporation from the Junction $J_{1,2}$.

At this point, Zone 1 behaves like an open end wedge pore, and desorption follows the same path as desorption from a completely filled pore.

Adsorption scanning is only possible from the state points in the shallow segment of the desorption boundary (B_2B_3). Interestingly, the adsorption scanning curve proceeds along a different path from the desorption scanning curve through gradual increases in density at the junctions and sharp condensations in the zones.

The snapshots shown in Figure 5 corroborate the discussion made above and are supported by the local density distributions along the pore at various points on the desorption scanning curve in Figure 6.

For the purpose of comparison, we include the local density distribution for the completely filled pore as a reference (top

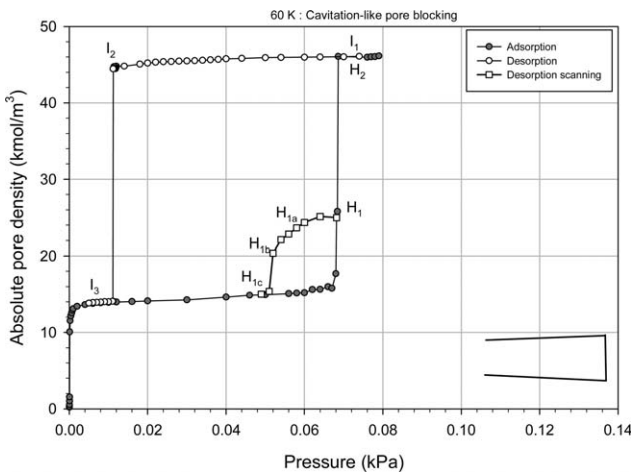

Figure 7. The adsorption–desorption isotherm and the desorption scanning curve in the wedge pore with its wide end closed at 60 K.

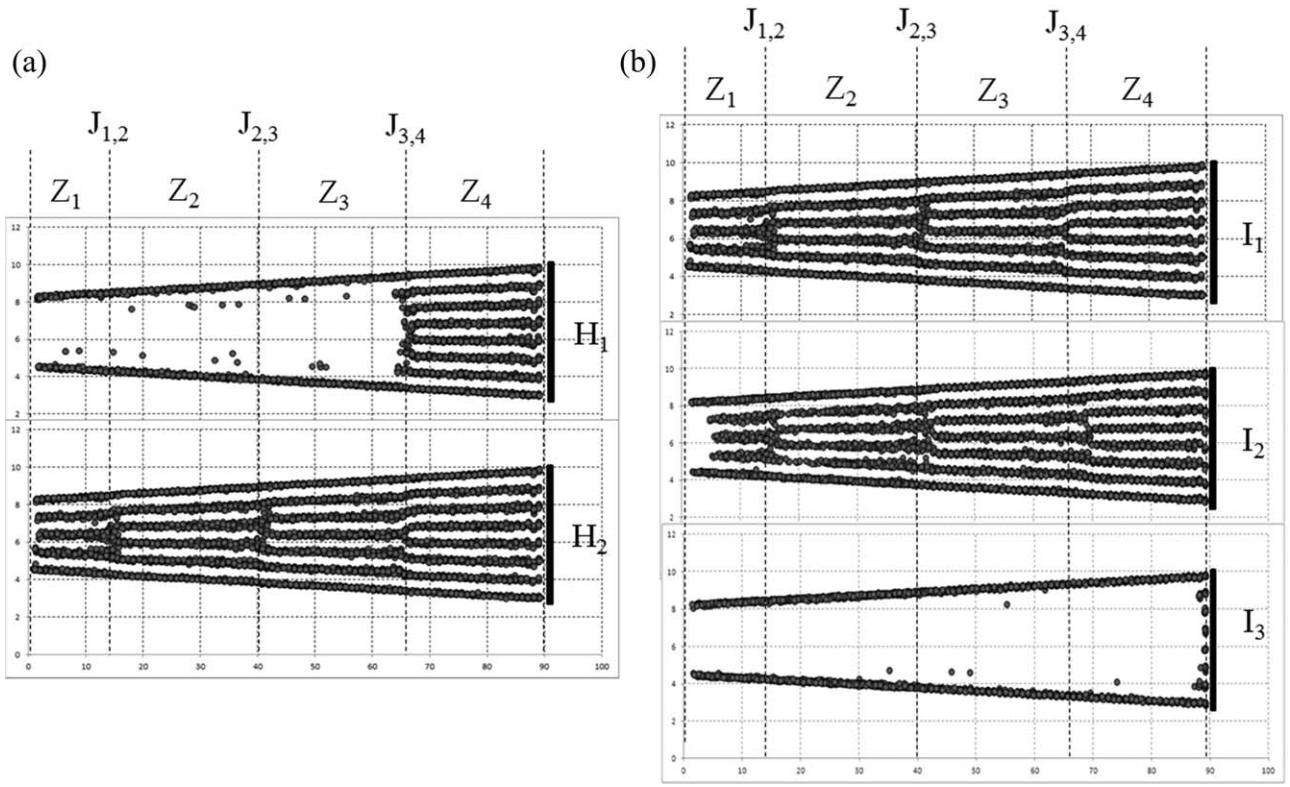

Figure 8. Snapshots in the wedge pore along the adsorption–desorption isotherm at 60 K.

H_1, H_2, and I_1–I_3 correspond to the points marked on the isotherm in Figure 7.

black curve labeled A_4). A number of features may be noted in Figure 6:

1. the Zones are identified as peaks and Junctions as troughs;
2. there is a sharp decrease in the density at the pore mouth;
3. the adsorbate becomes highly structured at the closed end (Zone 4) when the pore is completely filled as shown by the oscillations in the axial distribution.

As the desorption scanning starts from Point A_2'', we see that the axial distribution traces the zones and junctions until the Zone 1 becomes an open end wedge pore (Point A_{2d}). Furthermore, we also note a small decrease in density as pressure is decreased (see the enlargement in Figures 6b, c).

77 K. The adsorption–desorption isotherms at 77 K, including the scanning curves within the hysteresis loop, have been studied in our previous work.[26] The mechanisms for hysteresis and scanning are the same as those discussed for 70 K in the last section. The only difference between the two temperatures is that there are three steps instead of two at 77 K; these steps correspond to condensation in Z_1 and Z_2 (Points C_1C_2), Z_3, and Z_4, respectively.

87 K. Adsorption at 87 K is different from that at 70 or 77 K. Condensation occurs first in Z_1, and follows the same mechanism as in the open end wedge pore (F_1F_2 in Figure 4). This is followed by the gradual filling of Zones 2 and 3 by the advance of the meniscus into the pore interior. At this point, Zone 4 behaves as a cavity, and the usual condensation in the cavity follows when pressure is further increased. Desorption follows a typical cavitation mechanism with the evaporation of condensate from Zones 2 to 4, followed by desorption from an open end pore at Zone 1. The desorption scanning as well as the adsorption scanning are reversible because, if we start at any state point on the segment where gradual change is seen on either boundary, the system scans a gradual path without crossing any section where sharp change occurs. This is distinct from the observations made at 70 and 77 K.

The observed behavior of the scanning curves for temperatures between 70 and 87 K can be summarized as follows: Starting from any state on the shallow segment of either adsorption or desorption boundary, the system follows the shallow segment until it reaches a state point joining the shallow segment and the sharp segment. At this point, the system scans across the interior of the hysteresis loop along different paths for desorption scanning and adsorption scanning; for the former, there is a gradual variation in density in the zone and a sharp change in density at the junction, while for the latter, there is a gradual variation in density at the junction and a sharp change in the zone. One important feature is that the desorption scanning curve is always terminated at the cavitation point.

Cavitation-like pore blocking at 60 K

At 60 K, cavitation-like pore blocking is the controlling mechanism of evaporation from a completely filled pore; the adsorption–desorption isotherm and a desorption scanning curve at this temperature are presented in Figure 7. There are several differences compared with the higher temperatures where cavitation is the controlling mechanism for evaporation. The first distinction is the initial formation of a meniscus. At the higher temperatures (70–87 K), the meniscus was formed at the small pore mouth, resulting from the condensation in Zone 1, but at 60 K, adsorption proceeds by an initial molecular layering on the pore walls and the closed end, followed by condensation in Zone 4 to reach Point H_1 in Figure 7. At this point, adsorption passes through a very small segment of

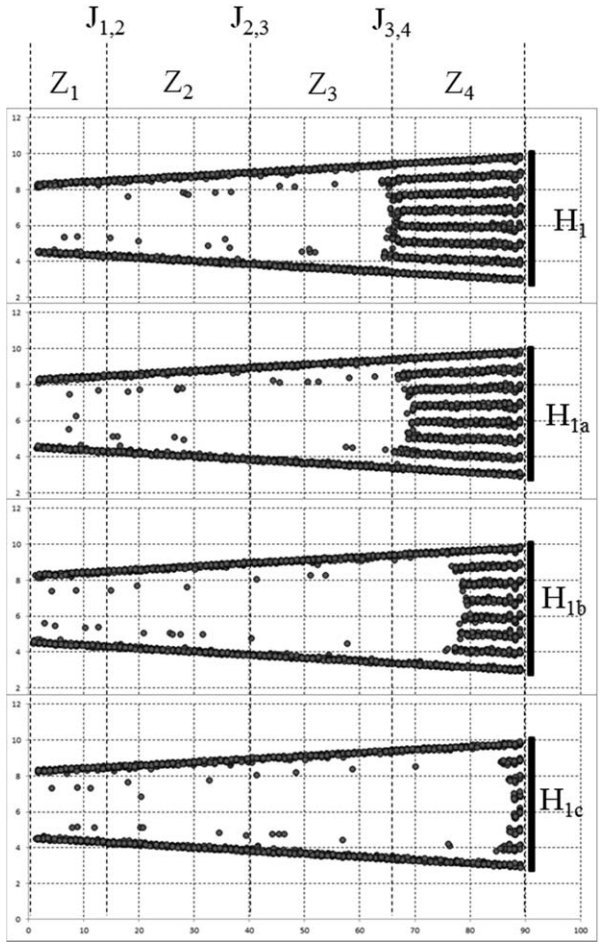

Figure 9. Snapshots in the wedge pore along the desorption scanning curve.

Points H_1 to H_{1c} are marked on the isotherm in Figure 7.

gradual change to fill Junction $J_{3,4}$, after which the second condensation fills the remaining volume of the pore to reach Point H_2. The snapshots in Figure 8 illustrate typical molecular configurations at Points H_1 and H_2.

On desorption from a completely filled pore, a meniscus is formed at the pore mouth and as the meniscus recedes into the pore interior, the adsorbate is increasingly exposed to the bulk gas and is stretched. When Point I_2 has been reached, the adsorbate evaporates from the pore, leaving thin layers of adsorbate on the pore walls and at the closed end. This behavior is typical of cavitation-like pore blocking which has been well known for a long time.[36]

At 60 K, it is possible to initiate a desorption scanning curve from Point H_1 on the adsorption boundary. At this point, Zone 4 is filled and the Junction $J_{3,4}$ is partially filled. As the pressure is reduced, the meniscus recedes (see Figure 9) with only a small decrease in density (H_1 to H_{1a}), because of the strong cohesion of the adsorbate, until Point H_{1b} has been reached when there is a sharp change in density to H_{1c} because: (1) the pressure is low enough; (2) the adsorbate has been stretched; and (3) the pore width at the position of the meniscus has increased. The most interesting observation in this case is that the desorption scanning curve leaves a point (H_1) on the adsorption boundary, and then returns to the same boundary at Point H_{1c}, which is far away from the lower closure point.

The main reason why the desorption scanning curve returns to the same boundary is because the scanning path is equivalent to a desorption from a short closed end pore for which the desorption can be effected at a higher pressure than for a longer closed end pore, in which the adsorbed fluid is more cohesive once the pore is filled.[37] The axial local density distributions in Figure 10 provide further evidence of the way in which the molecular structure of the adsorbate changes along the scanning curve. When the pore is full (Point H_2), there are multiple peaks in the zones indicative of a structured adsorbate induced by the closed end at this low temperature. At Point H_1, where the desorption scanning curve starts the

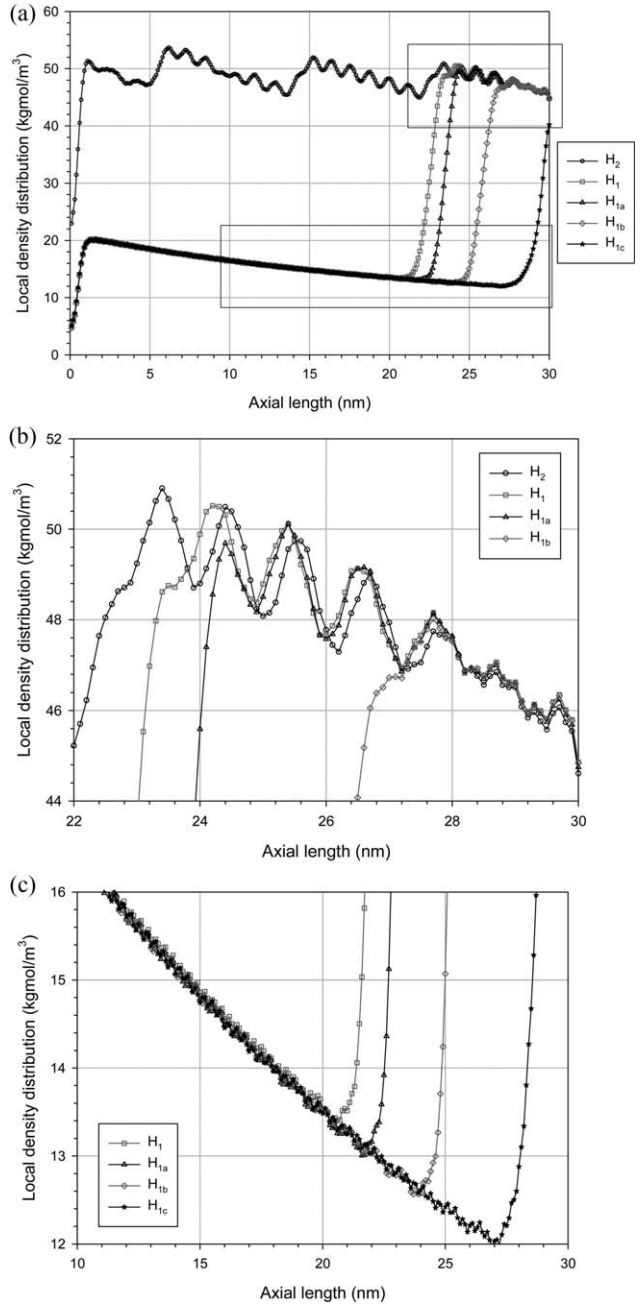

Figure 10. (a) Local density distributions in the wedge pore at 60 K. (b) and (c) are the enlargments of the filled and emptied phases, respectively. Points H_1 to H_{1c} are marked on the isotherm in Figure 7.

adsorbate in Zone 4 is not as cohesive as that in the filled pore (Point H_2), and therefore, the desorption scanning terminates at a higher pressure, that is, the scanning returns to the same boundary.

Conclusions

We have used GCMC simulation at several temperatures to investigate scanning curves within the hysteresis loop of argon adsorption–desorption isotherms, for a wedge-shaped pore with its wide end closed, to study the role of cavitation and pore blocking on scanning curves. The molecular packing of the adsorbate alternates between zones, where it is essentially commensurate with the pore width, and junctions where it is incommensurate and highly disordered. When the mechanism of evaporation is cavitation, the desorption scanning curve proceeds via a gradual decrease of density in the zones and sharp evaporation from the junctions, before reaching the lowest density on the cavitation branch. The opposite behavior is observed for adsorption scanning, where the scanning curve follows a sequence of gradual density increase in a junction and sharp condensation in the zones. When pore blocking is the controlling mechanism, the desorption scanning proceeds by recession of the meniscus, and the scanning curve returns to the same branch (i.e., the adsorption boundary curve) at a point which is at a far higher pressure than the lower closure point. This phenomenon has not been noted previously in the literature.

Acknowledgments

This work is supported by the Australian Research Council. The authors also acknowledge the support from the Thailand Research Fund (Contract no. TRG5780126) and the Internationalization for Research University (IRU) of Naresuan University.

Literature Cited

1. Horikawa T, Do DD, Nicholson D. Capillary condensation of adsorbates in porous materials. *Adv Colloid Interface Sci*. 2011;169:40–58.
2. Brunauer S, Mikhail RS, Bodor EE. Pore structure analysis without a pore shape model. *J Colloid Interface Sci*. 1967;24:451–463.
3. Brunauer S, Mikhail RS, Bodor EE. Some remarks about capillary condensation and pore structure analysis. *J Colloid Interface Sci*. 1967;25:353–358.
4. Mikhail RS, Brunauer S, Bodor EE. Investigations of a complete pore structure analysis: II. Analysis of four silica gels. *J Colloid Interface Sci*. 1968;26:54–61.
5. Mason G. The effect of pore space connectivity on the hysteresis of capillary condensation in adsorption-desorption isotherms. *J Colloid Interface Sci*. 1982;88:36–46.
6. Seaton NA. Determination of the connectivity of porous solids from nitrogen sorption measurements. *Chem Eng Sci*. 1991;46:1895–1909.
7. Liu H, Zhang L, Seaton NA. Determination of the connectivity of porous solids from nitrogen sorption measurements. II. Generalisation. *Chem Eng Sci*. 1992;47:4393–4404.
8. Liu H, Zhang L, Seaton NA. Sorption hysteresis as a probe of pore structure. *Langmuir*. 1993;9:2576–2582.
9. Liu H, Seaton NA. Determination of the connectivity of porous solids from nitrogen sorption measurements. III. Solids containing large mesopores. *Chem Eng Sci*. 1994;49:1869–1878.
10. Nguyen PTM, Fan C, Do DD, Nicholson D. On the cavitation-like pore blocking in ink-bottle pore: evolution of hysteresis loop with neck size. *J Phys Chem C*. 2013;117:5475–5484.
11. Fan C, Do DD, Nicholson D. Condensation and evaporation in capillaries with nonuniform cross sections. *Ind Eng Chem Res*. 2013;52:14304–14314.
12. Nguyen PTM, Do DD, Nicholson D. Pore connectivity and hysteresis in gas adsorption: a simple three-pore model. *Colloids Surf A: Physicochem Eng Asp*. 2013;437:56–68.
13. Reichenbach C, Kalies G, Enke D, Klank D. Cavitation and pore blocking in nanoporous glasses. *Langmuir*. 2011;27:10699–10704.
14. Morishige K. Adsorption hysteresis in ordered mesoporous silicas. *Adsorption*. 2008;14:157–163.
15. Ravikovitch PI, Neimark AV. Experimental confirmation of different mechanisms of evaporation from ink-bottle type pores: equilibrium, pore blocking, and cavitation. *Langmuir*. 2002;18:9830–9837.
16. Klomkliang N, Do DD, Nicholson D. Effects of temperature, pore dimensions and adsorbate on the transition from pore blocking to cavitation in an ink-bottle pore. *Chem Eng J*. 2014;239:274–283.
17. Cychosz KA, Guo X, Fan W, Cimino R, Gor GY, Tsapatsis M, Neimark AV, Thommes M. Characterization of the pore structure of three-dimensionally ordered mesoporous carbons using high resolution gas sorption. *Langmuir*. 2012;28:12647–12654.
18. Rasmussen CJ, Vishnyakov A, Thommes M, Smarsly BM, Kleitz F, Neimark AV. Cavitation in metastable liquid nitrogen confined to nanoscale pores. *Langmuir*. 2010;26:10147–10157.
19. Monson PA. Understanding adsorption/desorption hysteresis for fluids in mesoporous materials using simple molecular models and classical density functional theory. *Microporous Mesoporous Mater*. 2012;160:47–66.
20. Grosman A, Ortega C. Influence of elastic deformation of porous materials in adsorption-desorption process: a thermodynamic approach. *Phys Rev B*. 2008;78:085433.
21. Cimino R, Cychosz KA, Thommes M, Neimark AV. Experimental and theoretical studies of scanning adsorption–desorption isotherms. *Colloids Surf A: Physicochem Eng Asp*. 2013;437:76–89.
22. Esparza JM, Ojeda ML, Campero A, Dominguez A, Kornhauser I, Rojas F, Vidales AM, Lopez RH, Zgrablich G. N2 sorption scanning behavior of SBA-15 porous substrates. *Colloids Surf A: Physicochem Eng Asp*. 2004;241:35–45.
23. Everett DH, Smith FW. A general approach to hysteresis. Part 2: development of the domain theory. *Trans Faraday Soc*. 1954;50:187–197.
24. Tompsett GA, Krogh L, Griffin DW, Conner WC. Hysteresis and scanning behavior of mesoporous molecular sieves. *Langmuir*. 2005;21:8214–8225.
25. Morishige K. Hysteresis critical point of nitrogen in porous glass: occurrence of sample spanning transition in capillary condensation. *Langmuir*. 2009;25:6221–6226.
26. Klomkliang N, Do DD, Nicholson D. Hysteresis loop and scanning curves of argon adsorption in closed end wedge pores. *Langmuir*. 2014;30:12879–12887.
27. Sarkisov L, Monson PA. Lattice model of adsorption in disordered porous materials: mean field density functional theory and Monte Carlo simulations. *Phys Rev E*. 2001;65:011202.
28. Allen MP, Tildesley TP. Computer Simulation of Liquids. Oxford, UK: Clarendon, 1987.
29. Bruschi L, Carlin A, Mistura G. Complete wetting on a linear wedge. *Phys Rev Lett*. 2002;89:166101.
30. Bruschi L, Carlin A, Parry AO, Mistura G. Crossover effects in the wetting of adsorbed films in linear wedges. *Phys Rev E*. 2003;68:021606.
31. Parry AO, Rascón C. The trouble with critical wetting. *J Low Temp Physics*. 2009;157:149–173.
32. Bojan MJ, Steele WA. Computer simulation of physisorption on a heterogeneous surface. *Surf Sci*. 1988;199:L395–L402.
33. Bojan MJ, Steele WA. Computer-simulation of physisorbed kr on a heterogeneous surface. *Langmuir*. 1989;5:625–633.
34. Bojan MJ, Steele WA. Computer-simulation of physical adsorption on stepped surfaces. *Langmuir*. 1993;9:2569–2575.
35. Nickmand Z, Do DD, Nicholson D, Aghamiri SF, Khozanie MRT, Sabzyan H. GCMC simulation of argon adsorption in wedge shaped mesopores of finite length. *Adsorption*. 2013;19:1245–1252.
36. McBain JW. An explanation of hysteresis in the hydration and dehydration of gels. *J Am Chem Soc*. 1935;57:699–700.
37. Fan C, Do DD, Nicholson D. On the hysteresis of argon adsorption in a uniform closed end slit pore. *J Colloid Interface Sci*. 2013;405:201–210.

Manuscript received Dec. 7, 2014, and revision received Apr. 14, 2015.